Int. J. Heat Mass Transfer. Vol. 18, pp. 337–339. Pergamon Press 1975. Printed in Great Britain

A SIMPLIFIED MODEL FOR PREDICTING OVERALL HEAT-TRANSFER COEFFICIENTS FOR CAVITY BEARING FLOW OBSTRUCTIONS

H. G. RIGO* and J. J. STUKEL†

(*Received* 26 *March* 1974 *and in revised form* 25 *June* 1974)

NOMENCLATURE

P, T/T_w;
T, absolute temperature;
h, convective heat-transfer coefficient;
k, thermal conductivity;
m, Euler number, defined in text;
f, defined in text;
q, heat flux;
Q, heat transfer;
X, dimension in the direction of flow along the wedge;
C_p, heat capacity;
Nu, Nusselt number, hx/k;
Pr, Prandtl number, $\frac{C_p\mu}{k}$;
Re, Reynolds number, $\frac{UDc}{v}$;
U_∞, free stream velocity;
ρ, density;
θ, temperature ratio or nondimensional mass flux;
v, kinematic viscosity;
μ, dynamic viscosity;
ψ, stream function.

Subscript

w, wall.

INTRODUCTION

A NOVEL combination particulate pollution control and heat-transfer element has recently been proposed [1]. The active element is a modified boiler tube. It has been found that by modifying the shape of a boiler tube to the configuration shown in Fig. 1, particulate removal can be realized without suffering any significant penalty in heat transfer performance. Since most boiler installations have a large array of boiler tubes, the net effect of replacing existing boiler tubes with the modified tubes is that the array of modified boiler tubes acts as a large filter in this new design. Provisions are made in the design to effect continuous particle removal after collection.

The prediction of the heat-transfer coefficient for this element requires the description of the carrier gas flow field through laterally disposed boiler tubes such as the ones displayed in Fig. 1. Since the front opening cavity introduces a confined secondary flow into the solution, the complete, steady state, incompressible isothermal Navier–Stokes equations had to be solved. The complete solution of the Navier–Stokes equation for the tubular array for Reynolds numbers up to 250 000 was solved by Rigo [1]. Given the flow field, the second prediction problem was to estimate the heat-transfer effectiveness of a cavity bearing tube in the array. A method for predicting the heat-transfer characteristics for this complicated geometry using a simple model is given in the following section.

*U.S. Army Corps of Engineers, Construction Engineering Research Laboratory, Champaign, Illinois 61820, U.S.A.

†Associate Professor of Civil Engineering and Mechanical Engineering, University of Illinois at Urbana–Champaign, Urbana, Illinois 61801, U.S.A.

HEAT-TRANSFER MODEL

The heat-transfer model reported in this note results from coupling the equivalent wedge similarity procedure with the Chapman–Korst [2–4] flow model to predict the heat-transfer characteristics of a complicated body containing a cavity. In particular, this new model is applied to a geometry consisting of a cavitated front-step section.

Applying the Chapman–Korst model to the cavitated tube dictates that the heat transfer be broken down into four zones. These are a leading boundary layer before the cavity is reached, the shear layer over the face of the cavity, a trailing boundary layer downstream of the cavity, and a boundary layer developed within the cavity itself. Referring to Fig. 2, it is noted that the heat transfer can be resolved into three major components. First, heat is transferred through the leading boundary layer. Second, heat is transferred through the shear layer into the cavity flow and then from the cavity flow through the cavity boundary layer to the object. Third, heat is transferred through the following boundary layer to the flow obstruction.

The computational procedure employed was to first calculate the heat transferred through the leading and trailing boundary layers using the equivalent wedge flow similarity solution (see Appendix A). The computation was performed by first calculating the Euler number using the development length of the boundary layer to the point in question, the velocity gradient parallel to the body at that point and the tangential velocity outside the shear layer. Given the Euler number and the infinity to wall temperature ratio, the temperature gradient at the wall was evaluated from the solution of the momentum and energy equations written for wedge flows at the boundary layer (see Appendix A). The local heat-transfer coefficient and the local heat flux was then computed from a heat balance from the gas to the tube surface. The results of the heat flux computation were integrated numerically along the surface to obtain the total heat flux.

The evaluation of the heat transfer rate through the cavity proceeds in a similar manner. First, the cavity flow-bulk flow innerface was located from the numerical solution of the velocity field as discussed earlier. This stream line was treated as an artificial surface. The reference temperature for the "wall" was assigned as an artificial bulk temperature. The heat-transfer rate through the mixing layer and the

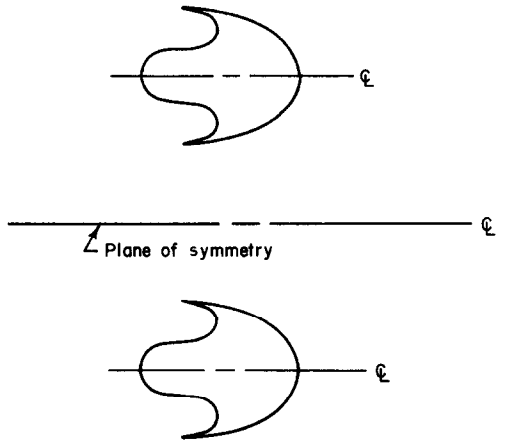

FIG. 1. Two bodies symmetrically disposed about a plane.

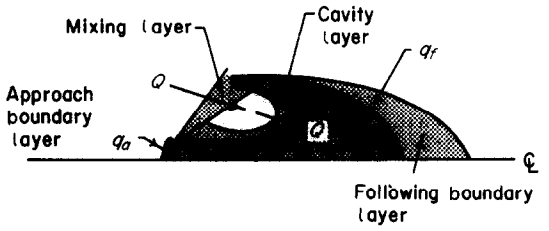

FIG. 2. Application of the equivalent wedge similarity solution to the Chapman–Korst model.

cavity boundary layer was computed next. The artificial cavity temperature was then adjusted until the heat flux into and out of the cavity were matched.

The heat-transfer rate through the leading boundary layer, the cavity, and the following boundary layer are all summed. This flux, divided by the temperature difference between the bulk fluid and the heat-transfer element, allowed the boiler tube heat transfer coefficient to be calculated.

HEAT TRANSFER EXPERIMENT

The overall heat-transfer rate predicted by the model was experimentally verified for approach velocities of 18·5 and 33·6 m/s. The heat-transfer coefficient of the rod was obtained experimentally from an energy balance in the usual manner.

The predicted values of the heat-transfer coefficient at both the low and high speed were within 6 per cent of the experimentally determined values. This error is within the nominal ± 7 per cent assigned to convective heat-transfer coefficients.

RESULTS AND CONCLUSIONS

The theoretical and experimental results indicate that the heat-transfer contribution of the cavity is small compared with the contribution from the nose portion and the following edge. The theoretical model predicts about 15 per cent of the heat transfer through the nose and 80 per cent through the trailing edge.

The coupling of the Chapman–Korst model and the equivalent wedge flow similarity model permits thermal evaluation of the performance of cavity bearing flow obstructions. Current use of the Chapman–Korst model has generally been limited to situations where the cavity boundary layers can be approximated by plate type flows. A solid body rotating core type flow has been assumed for the contained fluid. The novel coupling of the models permits flow patterns in the cavity other than this core type rotation. The need to relax this approximation in heretofore analyzed systems has been minimal since a solid body rotating core is a good approximation to the real system [5]. With cavities opening into the flow, however, significant distortion of the core can occur and another means of establishing the mixing layer is needed. The proposed coupling of the Chapman–Korst cavity flow model and the equivalent wedge flow similarity solution can fulfill that need.

REFERENCES

1. H. G. Rigo, An extended evaluation of a particulate precipitating heat transfer surface, Ph.D. Thesis, University of Illinois at Urbana–Champaign (1973).
2. H. H. Korst, Comments on the effect of boundary layer on sonic flow on abrupt cross-section area change, *J. Aeronaut. Sci.* **21**, 568–569 (1954).
3. H. H. Korst, A theory for base pressures on transonic and supersonic flow, *J. Appl. Mech.* **23**, 593–600 (1956).
4. D. R. Chapman, D. M. Kuehn and H. K. Larson, Investigation of separated flows in supersonic and subsonic streams with emphasis on the effect of transition, NACA Report 1356 (1958).
5. F. Pan and A. Acrives, Steady flows in rectangular cavities, *J. Fluid Mech.* **87**, 643 (1967).
6. E. Eckert, Die berechnung des warmeubergangas in der laminaren grenzschicht unstromter korper, *Forsch. Geb. IngWes.* **1**, 13 (1942).
7. W. B. Brown and J. N. Livingood, Solutions of laminar boundary layer equations which result in specific weight flow profiles locally exceeding free stream values, NACA T.N. 2600 (1952).
8. E. Eckert and J. N. Livingood, Method for calculating laminar heat transfer in air flow around cylinders or arbitrary cross-section, NACA Report 1118 (1953).
9. J. H. Keenan and J. Kays, *Gas Tables*. John Wiley, New York (1947).

APPENDIX A

Following the work of Eckert [6] and others [7,8], the energy and momentum equations for the flow outside the boundary layer of a wedge can be written as follows:

$$-\theta'' = \frac{m+1}{2}(Pr)_w P^{-0.66}\theta' f + 0.85\left(\frac{T_\infty}{T_w} - 1\right)P^{-1}\theta'^2$$

$$f''' = mP^{-0.7}f'^2 - \frac{m+1}{2}P^{-1.07}ff'\theta' - \frac{m+1}{2}P^{-0.7}ff''$$
$$-m\frac{T_w}{T_\infty}P^{-1}f'\theta'' - \left(\frac{T_\infty}{T_w} - 1\right)P^{-1}f'\theta'' - 2.07\left(\frac{T_\infty}{T_w} - 1\right)$$
$$\times P^{-1}f''\theta' - 0.7\left(\frac{T_\infty}{T_w} - 1\right)^2 P^{-2}f'\theta'^2$$

where

$$\theta = \frac{T - T_w}{T_\infty - T_w}; \quad P = \frac{T}{T_w}; \quad f = \frac{\psi}{\sqrt{\left(\frac{\mu_w X U_\infty}{\rho_w}\right)}};$$

$$\eta = Y\sqrt{\left(\frac{\rho_w U_\infty}{\mu_w X}\right)}$$

$$U_\infty \propto X^m; \quad m = \frac{X\left(\frac{dU}{dX}\right)}{U_\infty};$$

the prime denotes differentiation with respect to η and following the experimental work of Keenan and Kays [9]

$$\mu \propto T^{0.7}; \quad K \propto T^{0.85}; \quad C_p \propto T^{0.19}; \quad \rho \propto \frac{1}{T}.$$

The boundary conditions are

$$\eta = 0; \quad f = 0; \quad f' = 0; \quad \theta = 0$$

and, as the edge of the boundary layer is approached

$$\theta \to 1; \quad \theta' \to 0; \quad \theta'' \to 0$$

and

$$f \to \infty; \quad f' \to \frac{T_w}{T_\infty}, \quad f'' \to 0.$$

Int. J. Heat Mass Transfer. Vol. 18, pp. 339–341. Pergamon Press 1975. Printed in Great Britain

TEMPERATURE DISTRIBUTIONS AND HEAT-TRANSFER CHARACTERISTICS OF A VEE-FIN ARRAY

V. R. MEGLER
Mechanical Engineering Department, University of Melbourne, Victoria, Australia

(*Received* 5 *February* 1974 *and in revised form* 6 *June* 1974)

NOMENCLATURE

- b, half thickness of fin;
- h, mean convective film coefficient over fin surface;
- k, thermal conductivity;
- Nu, mean Nusselt number;
- Re, Reynolds number;
- T, surface temperature;
- T_1, temperature at the end of fin;
- T_s, the free stream temperature of air;
- ϑ, temperature difference $(T - T_s)$;
- ϑ_1, temperature difference $(T_1 - T_s)$.

INTRODUCTION

THE DESIGN of a compact heat exchanger relies on the high surface area density, which is obtained by compact heat-transfer surfaces. The one used extensively in radiator design is the plate fin design with triangular or square passages using interconnected fins [1].

The vee-fin design is favored for radiators, since it is easy to manufacture. A long strip of metal is formed into appropriate shape and then attached to the flattened tubes, so forming a continuous array of short triangular passages. This triangular passage consists of the flattened tube (primary surface) and the two lateral sides, i.e. the fins or the secondary surfaces.

The heat flux from the secondary surface, i.e. fin, is a function of the surface temperature of the fin, the fluid temperature and the flow characteristics. To evaluate the fin surface temperature distribution the fin material conductivity, the film coefficient and the fin geometry must be known.

The purpose of this investigation was to obtain more information about temperature distribution and film coefficient on the surface of a fin, forming a part of the triangular passage and exposed to air flow.

EXPERIMENTAL APPARATUS

The test section of 0·3048 × 0·1524 m (12 × 6 in) and 0·0254 m (1 in) deep consisted of an array of three triangular passages, each 0·1524 m (6 in) high with base of 0·1016 m (4 in). The fins separating the passages were 0·002 m ($\frac{5}{64}$ in) thick, heated at the base and at the apex of the passage.

The central triangular passages were used for temperature measurements.

The thermocouples were fixed at 0·019 m (0·75 in) intervals alternatively at top and bottom surface of the two fins forming the central triangular passage.

Each thermocouple was soldered into a small slit at the surface. The surface was then sanded smooth so as not to create a disturbance to the flow. The thermocouple leads were neatly tucked to form the trailing edge of the fin.

The test section was mounted into the test rig, consisting of a long rectangular duct, forming the experimental section. The base and the apex of the triangular array of test section were flush with the rectangular duct. The wall temperatures T_1 were measured at the base and at the apex of the triangular section. The first reading was taken after stable conditions had been maintained for 15 min and after interval of further 10 min the second reading.

The tests were made for four different wall temperatures for each of which six Reynolds numbers conditions were employed.

The differences between any two readings at the same point were of the order of approximately 0·25°C.

THEORY AND EXPERIMENTAL RESULTS

Considering the radiator geometry as an array of short triangular passages, the sides of the passages being the fins. Each fin can be presented as rectangular plate of length $2l$ and thickness $2b$ of uniform thermal conductivity, k, receiving the heat from two heat sources located at ends and at same temperature T_1. The heat is dissipated from its two surfaces to an ambient air at temperature T_s. Assuming the value of mean film coefficient, h, to be the same for the two surfaces of the fin, the surface temperature, T, is given by the equation

$$\vartheta = \vartheta_1 \frac{\cosh mx}{\cosh ml} \tag{1}$$

where

$$\vartheta = T - T_s, \quad \vartheta_1 = T_1 - T_s \quad \text{and} \quad m = h/2kb \quad [2\text{–}4].$$

The surface temperature distribution was measured for the